HHS Public Access

Author manuscript

Comput Biol Med. Author manuscript; available in PMC 2016 October 01.

Published in final edited form as:

Comput Biol Med. 2015 October 1; 65: 161–167. doi:10.1016/j.compbiomed.2015.08.005.

Assessing the Atrial Electromechanical Coupling during Atrial Focal Tachycardia, Flutter, and Fibrillation using Electromechanical Wave Imaging in Humans

Jean Provost[1], **Alexandre Costet**[1], **Elaine Wan**[2], **Alok Gambhir**[2], **William Whang**[2], **Hasan Garan**[2], and **Elisa E. Konofagou**[1,3,*]

[1]Department of Biomedical Engineering, Columbia University, New York, NY, 10032

[2]Department of Medicine, Division of Cardiology, Columbia University, New York, NY, 10032

[3]Department of Radiology, Columbia University, New York, NY, 10032

Abstract

Minimally-invasive treatments of cardiac arrhythmias such as radio-frequency ablation are gradually gaining in importance in clinical practice but still lack a noninvasive imaging modality which provides insight into the source or focus of an arrhythmia. Cardiac deformations imaged at high temporal and spatial resolution can be used to elucidate the electrical activation sequence in normal and paced human subjects non-invasively and could potentially aid to better plan and monitor ablation-based arrhythmia treatments. In this study, a novel ultrasound-based method is presented that can be used to quantitatively characterize focal and reentrant arrhythmias. Spatio-temporal maps of the full-view of the atrial and ventricular mechanics were obtained in a single heartbeat, revealing with otherwise unobtainable detail the electromechanical patterns of atrial flutter, fibrillation, and tachycardia in humans. During focal arrhythmias such as premature ventricular complex and focal atrial tachycardia, the previously developed electromechanical wave imaging methodology is hereby shown capable of identifying the location of the focal zone and the subsequent propagation of cardiac activation. During reentrant arrhythmias such as atrial flutter and fibrillation, Fourier analysis of the strains revealed highly correlated mechanical and electrical cycle lengths and propagation patterns. High frame rate ultrasound imaging of the heart can be used non-invasively and in real time, to characterize the lesser-known mechanical aspects of atrial and ventricular arrhythmias, also potentially assisting treatment planning for intraoperative and longitudinal monitoring of arrhythmias.

Keywords

Echocardiography; electrophysiology mapping; imaging; arrhythmia; premature ventricular contraction

[*]Corresponding author: Department of Biomedical Engineering, Columbia University, 1210 Amsterdam Avenue, New York, NY 10027, Tel: 212-854-9661/212-342-0863, Fax: 212-342-5773, ek2191@columbia.edu.

Introduction

Atrial arrhythmias are a major cause of morbidity and mortality worldwide. Extensive research underscores the important role of mechanical factors such as fiber orientation (Tobón et al., 2013), chamber size and wall tension in the onset and perpetuation of atrial arrhythmia (see (Jong et al., 2011) for a review) and how existing echocardiographic measurements can be used to characterize atrial arrhythmias (Caglar et al., 2012; Mirza et al., 2011; Zhang et al., 2008). Yet, there is little information on the 2-D spatio-temporal evolution of the local deformations of the atria during e.g., focal tachycardia, flutter, and fibrillation.

Over the last few years, ultrasound imaging has been undergoing important technical improvements with the advent of software-based systems that allow ultra-high frame rates: 2000–5000 frames/s are achieved by using defocussed transmissions, as opposed to the 50–200 frames/s used in commercial clinical systems, for the depths needed in transthoracic cardiac applications (Bercoff et al., 2004; Bruneel et al., 1977; Delannoy et al., 1979; Honjo et al., 2010; Papadacci et al., 2014; Provost et al., 2014, 2011c). Such high frame rates allow unprecedented temporal resolution, and, perhaps most importantly, a five-fold improvement in the signal-to-noise ratio of cardiac motion and deformation mapping (Provost et al., 2012). Using such techniques, we have recently shown that mapping the transient strains occurring in response to the electrical activation, i.e., the electromechanical wave, can be used to map the transmural activation sequence of the normal and abnormal heart (Provost et al., 2011a, 2011b, 2010) and to locate pacing sites in patients undergoing cardiac resynchronization therapy (Provost et al., 2013).

Expanding on this approach, for the purposes of this study, we have developed novel methodologies applied to the study of the mechanical behavior of the atria during four specific types of cardiac arrhythmia, i.e., premature ventricular complex, focal tachycardia, atrial flutter and atrial fibrillation. We first show that while the previously developed approach of Electromechanical Wave Imaging (EWI) is apt at characterizing premature ventricular complex and focal tachycardia, which are focal rhythms, it failed at fully describing reentrant rhythms such as atrial flutter and fibrillation. To palliate this issue, we developed a novel technique for the description of electromechanical strains during reentrant rhythms based on the Fourier analysis. We introduced a single acquisition sequence that can be used for either standard EWI or for the Fourier analysis of electromechanical strains which constitutes this novel diagnostic tool namely ‘electromechanical activation mapping’, which can describe the electromechanical strains propagation patterns during both focal and reentrant arrhythmias. To our knowledge, no other previously reported study can characterize atrial strains during arrhythmia. We demonstrate that the local deformations of the atria are often closely correlated with their electrical activation and could be used to better assess the role of cardiac mechanics in arrhythmia and, potentially, to better plan ablation treatments and monitor their efficacy non-invasively and in real-time, longitudinally.

Methods

The study protocol was approved by the Institutional Review Board (IRB, protocol AAAA9333) of Columbia University, and written informed consent was obtained from all human subjects prior to scanning. All human subjects underwent a diagnostic ultrasound scan a few minutes to a few hours prior to an electroanatomic mapping and ablation procedures. The cardiac arrhythmias of the patients were confirmed during that procedure: premature ventricular complex (n=1), atrial flutter (n=5), focal atrial tachycardia (n=1), and atrial fibrillation (n=1). Patients for which ectopic foci were located outside the echocardiographic apical 4-chamber view were excluded. The total number of subjects was equal to 9, i.e., 8 patients and 1 control.

Strain maps were first generated using methods akin to the ones developed for single-heartbeat electromechanical wave imaging (EWI) (Provost et al., 2011c). More specifically, a Verasonics system with a 2.5-MHz probe was calibrated and customized to adhere to FDA standards both in terms of mechanical index and of spatial-peak-temporal-average intensity and was deemed a non-significant risk and approved for human use by the IRB of Columbia University. The ultrasound scan was composed of two sequences. First, a motion-estimation sequence, in which a circular ultrasonic wave was emitted with a virtual focus 10.2 mm behind the probe at 2000 fps during 2 s. Immediately following this sequence, a standard B-mode acquisition was performed during 1.5 s to accurately depict the heart anatomy. This additional sequence is necessary because the B-mode images obtained from the motion-estimation sequence provide low contrast due to the use of diverging waves and is thus of limited clinical use. Frames from the motion-estimation sequence were reconstructed by generating 128 beams in post-processing via a delay-and-sum algorithm with a reconstructed sampling frequency of 20 MHz. The motion-estimation rate and the motion-sampling rate were 1000 and 2000 fps, respectively. The window used for motion-estimation was of 9.2 mm with an overlap of 95.8% (window shift of 0.3 mm) and the kernel used for strain estimation was 4.9 mm. Beamforming, motion-estimation, strain estimation, spatial moving-average of the strains (12 mm by 10 lines), and the automated contour tracking technique were performed off-line using a Tesla GPU (Nvidia, Santa Clara, CA) and the Matlab parallel processing toolbox (The Mathworks, Nattick, MA) at a computing speed of 2.4 frames/s.

As high frame-rate mechanical data was acquired in patients with different types of rhythms, it became apparent that focal and reentrant arrhythmias had to be analyzed differently. Figure 1 and supplementary video 1 show the strains mapped in subjects who have sinus rhythm (Fig. 1a), atrial flutter (Fig. 1b), atrial fibrillation (Fig. 1c), and atrial focal tachycardia (Fig. 2d). In subjects in sinus rhythm, the strains in one location, e.g., one pixel in the LA, presented two main events over time that corresponded approximately to the beginning and the end of systole (Fig. 1a). In subjects in focal tachycardia, distinct events could also be identified. Therefore, by tracking the onset (i.e., the first zero-crossing) of these events for every pixel of the heart walls, isochrones maps can be generated. In atrial flutter patients, a similar location in the LA revealed periodic strains, which were, in some cases, strongly dominated by a single frequency (Fig. 1b). However, in a patient with atrial

fibrillation (Fig. 1c), multiple frequencies were observed, suggesting that an analysis based on the Fourier transform might be appropriate.

Therefore, in subjects who have focal rhythms such as sinus rhythm and focal tachycardia, the onset of contraction was determined as the first zero-crossing of the incremental strains occurring after the onset of the P-wave on the electrocardiogram (ECG), following the previously described EWI methodology (Provost et al., 2011b, 2010). Specifically, the EW was mapped using activation ciné-loops and isochrones maps obtained by detecting, the first time following activation onset on the ECG when the strains cross zero. In atria with reentrant arrhythmia, i.e., during flutter and fibrillation, a high-resolution Fourier transform was performed using a generalized Goertzel algorithm for efficient and optimal interpolation in Fourier space (Sysel and Rajmic, 2012) on 1.5-s long incremental strains signals for each individual pixel in the atria. The Goertzel algorithm provides is an efficient signal processing technique when a small portion of the spectrum is of interest. The open-source code made available in (Sysel and Rajmic, 2012) was adapted to run on the GPU but was otherwise used as-is. In order to compare them against conventional ECG measurements, frequencies were converted to cycle lengths, which will be referred to as mechanical cycle length (MCL) throughout. Peak MCL maps were then generated by selecting the MCL with the highest amplitude within the physiologically-relevant 100–330 ms range for each pixel. Peak cycle lengths histograms were then constructed and compared to the electrical cycle length measured directly during the mapping and ablation procedures. Figure 2 summarizes the two types of processing that were used for focal and non-focal rhythms.

Results

Focal rhythms

Figure 3 and supplementary video 2 show EWI ciné-loop and isochrones during focal rhythms. Fig. 2A shows the atria of a normal subject, with propagation from the RA to the LA. Fig. 2B shows the atria of a patient for which electrical mapping revealed a focal atrial tachycardia with a focus most likely located high in the left atrium (LA). However, electrical mapping of this patient was not completed in the LA. EWI shows electromechanical activation originating from the LA and propagating into both atria, after which further activation was detected in the ventricles.

Figures 3B and C show the isochrones obtained in a patient with frequent premature ventricular complexes. EWI was performed during sinus rhythm and during pre-ventricular contraction. The EWI isochrones obtained during sinus rhythm show propagation from the RA, into the LA and then into the ventricles, similar to the normal cases published previously (Provost et al., 2013, 2011b). When this patient underwent premature ventricular complex, the region that was activated early in the ventricle during sinus rhythm triggered the entire electromechanical activation sequence, i.e., from the ventricles to the atria.

Reentrant rhythms

Figure 4 shows the electromechanical behavior of a heart undergoing atrial flutter. Fig. 4A shows the peak MCL map, where a single MCL was clearly dominant, as illustrated by the

histogram of Fig. 4B, with the most common MCL being approximately 294 ms. When analyzing the phase of that MCL in Fourier space, we can observe a propagation pattern originating from the right atrium (RA) near the tricuspid valve towards the LA (Fig. 4C). The electrical cycle length was 283 ms, as shown on the intracardiac electrograms (Fig. 3D).

However, not all atrial flutter cases exhibited exactly the same pattern. Indeed, the majority of the flutter cases studied (4 out of 5) presented with two dominant frequencies, often separated between the left and right atria, whereas the electrophysiological data available indicated that only one reentrant circuit was present. Fig. 5A shows two examples of this behavior: peak MCL maps revealed two dominant frequencies, one mostly located in the RA, the other being mostly located in the LA. Notably, in all 5 cases, one of these two dominant MCL was very close to the electrical cycle length, as shown in Fig. 5B for the 5 atrial flutter cases we studied.

Figures 5C and D depict the results from one patient undergoing atrial fibrillation. The peak MCL map (Fig. 5C) reveals multiple clustered dominant frequencies. The separation into these dominant frequencies is quantified by the histogram (Fig. 5D).

Discussion

The objective of this study was to establish the feasibility of the novel technique of electromechanical activation mapping for the identification of the site and characterization of the mechanisms of cardiac rhythms during arrhythmia in humans, which may allow for optimization of treatment and clinical management. Current clinical practice relies on minimally invasive techniques to obtain precise maps of the activation of the atria and ventricles. Such techniques are costly, time-consuming, and carry some degree of risk, hence limiting the availability of complete activation maps before and after treatment but also during catheter procedures.

In this study, we have developed new methods for, and demonstrated initial feasibility of, electromechanical activation mapping during reentrant and focal arrhythmias. We reported, for the first time, imaging of the spatiotemporal mechanics of arrhythmias with high accuracy and spatial and temporal resolutions in a full field of view in humans. In all the cases we studied, it was possible to characterize an electromechanical propagation pattern or dominant mechanical cycle lengths, which were in turn closely associated with their electrophysiological equivalents.

Focal rhythms behaved similarly to the paced rhythms observed in previous studies (Provost et al., 2011b), i.e., with a single source of electromechanical activation located in the vicinity of the earliest electrical activation. Previous studies by our group have demonstrated the capability of EWI to characterize the propagation of the electromechanical activation from the sinus node in the atria and from the bundle branch terminates in the ventricles as well as during ventricular pacing (Provost et al., 2013). In this study, we demonstrated that electromechanical activation propagation patterns similar to pacing occurred in a patient during premature ventricular complexes, while in the same patient during sinus rhythm, the electromechanical activation sequence was similar to our previous results in normal

subjects(Provost et al., 2013). In a patient with atrial tachycardia, the electromechanical activation propagation pattern revealed a source located near the roof of the LA, in accordance with electrical mapping. This case is exemplary of a potential application of non-invasive, ultrasound-based, electromechanical activation mapping, which can be done during or prior to invasive procedures. Indeed, in this specific case, prior knowledge of an electromechanical source located in the LA could have contributed to clinical preparation as to whether transseptal access would need to be obtained and to the risk-benefit analysis performed to determine the best course of treatment, e.g., pharmacological vs ablation treatment.

During atrial flutter, the electromechanical activation maps were again closely correlated with their electrical counterpart, at least in part of the atrial tissue. Indeed, in one case, a single dominant frequency could be identified, and the phase of that frequency revealed a propagation direction from the cavotricuspid isthmus region to the RA and LA, as is expected during typical atrial flutters. In the four other cases, it was possible to identify two distinct behaviors in the atria: one part of the atria was contracting with the same frequency as the electrical activation, while another region did not. In other words, mapping the mechanics of the heart could identify regions in which the mechanical and electrical activities appeared to be decoupled. Further spatial fragmentation of the periodicity of the mechanics of the atria was observed during fibrillation. While a clear relevance to the clinical routine remains to be determined, it is a first step towards a better understanding of the atrial mechanics during arrhythmia and their potential role in the progression from flutter to fibrillation and vice versa.

Limitations of the techniques used in this study include the deformation of the atria caused by the onset of ventricular contraction and relaxation and could affect frequency analyses that are based on multiple activation cycles, especially given the relatively short acquisition time used in this study. Filtering techniques and the development of longer acquisition sequences are the object of on-going studies. Moreover, the number of patients in this feasibility study was limited, especially for the study of ectopic foci and was due in part to the 2-dimensionnal nature of the imaging technique used as ectopic foci located outside the standard echocardiographic views were excluded. Efforts in development of 4D EWI are currently ongoing by our group in order to overcome the aforementioned limitations of 2D methodologies.

While other technologies for non-invasive electrical mapping (Ramanathan et al., 2004) are gradually entering clinical practice, they are typically limited to the epicardium and assume an immobilized heart function. A mechanical assessment of the atria can be a valuable addition to the tools currently available to the electrophysiologist or interventional cardiologist. In the current clinical routine, echocardiograms are already performed on almost every arrhythmia patient, while other non-invasive electrical mapping techniques typically rely on time-consuming and costly high resolution CT or MRI scans. The electromechanical activation mapping presented in this study could in principle be obtained in conjunction with routine echocardiograms using the required sequences and techniques, highlighting the translational aspects of our approach.

In conclusion, mapping the electromechanical activity during arrhythmias non-invasively with real-time feedback can be used to better understand the role played by atrial mechanics in the evolution and perpetuation of arrhythmias and potentially be used for a reliable method predicting their site of origin and the mechanism and monitoring of interventions outcomes.

Supplementary Material

Refer to Web version on PubMed Central for supplementary material.

Acknowledgments

This study was supported in part by the National Institutes of Health (R01EB006042, R21HL096094, R01HL114358). J.P. was funded in part by the Heart Rhythm Society Clinical Research Award in Honor of Mark Josephson and Hein Wellens.

References

Bercoff J, Tanter M, Fink M. Supersonic shear imaging: a new technique for soft tissue elasticity mapping. IEEE Trans Ultrason Ferroelectr Freq Control. 2004; 51:396–409.10.1109/TUFFC.2004.1295425 [PubMed: 15139541]

Bruneel C, Torguet R, Rouvaen KM, Bridoux E, Nongaillard B. Ultrafast echotomographic system using optical processing of ultrasonic signals. Appl Phys Lett. 1977; 30:371–373.10.1063/1.89436

Caglar IM, Dasli T, Turhan Caglar FN, Teber MK, Ugurlucan M, Ozmen G. Evaluation of atrial conduction features with tissue Doppler imaging in patients with chronic obstructive pulmonary disease. Clin Res Cardiol Off J Ger Card Soc. 2012; 101:599–606.10.1007/s00392-012-0431-7

Delannoy B, Torguet R, Bruneel C, Bridoux E, Rouvaen JM, Lasota H. Acoustical image reconstruction in parallel-processing analog electronic systems. J Appl Phys. 1979; 50:3153–3159.10.1063/1.326397

Honjo Y, Hasegawa H, Kanai H. Two-Dimensional Tracking of Heart Wall for Detailed Analysis of Heart Function at High Temporal and Spatial Resolutions. Jpn J Appl Phys. 2010:49.

Jong AMD, Maass AH, Oberdorf-Maass SU, Veldhuisen DJV, Gilst WHV, Gelder ICV. Mechanisms of atrial structural changes caused by stretch occurring before and during early atrial fibrillation. Cardiovasc Res. 2011; 89:754–765.10.1093/cvr/cvq357 [PubMed: 21075756]

Mirza M, Caracciolo G, Khan U, Mori N, Saha SK, Srivathsan K, Altemose G, Scott L, Sengupta P, Jahangir A. Left atrial reservoir function predicts atrial fibrillation recurrence after catheter ablation: a two-dimensional speckle strain study. J Interv Card Electrophysiol Int J Arrhythm Pacing. 2011; 31:197–206.10.1007/s10840-011-9560-6

Papadacci C, Pernot M, Couade M, Fink M, Tanter M. High-contrast ultrafast imaging of the heart. IEEE Trans Ultrason Ferroelectr Freq Control. 2014; 61:288–301.10.1109/TUFFC.2014.6722614 [PubMed: 24474135]

Provost J, Gambhir A, Vest J, Garan H, Konofagou EE. A clinical feasibility study of atrial and ventricular electromechanical wave imaging. Heart Rhythm. 2013; 10:856–862.10.1016/j.hrthm.2013.02.028 [PubMed: 23454060]

Provost J, Gurev V, Trayanova N, Konofagou EE. Mapping of cardiac electrical activation with electromechanical wave imaging: An in silico-in vivo reciprocity study. Heart Rhythm. 2011a; 8:752–759.10.1016/j.hrthm.2010.12.034 [PubMed: 21185403]

Provost J, Lee WN, Fujikura K, Konofagou EE. Imaging the electromechanical activity of the heart in vivo. Proc Natl Acad Sci. 2011b; 108:8565–8570.10.1073/pnas.1011688108 [PubMed: 21571641]

Provost J, Lee WN, Fujikura K, Konofagou EE. Electromechanical Wave Imaging of Normal and Ischemic Hearts in Vivo. IEEE Trans Med Imaging. 2010; 29:625–635.10.1109/TMI.2009.2030186 [PubMed: 19709966]

Provost J, Nguyen VTH, Legrand D, Okrasinski S, Costet A, Gambhir A, Garan H, Konofagou EE. Electromechanical wave imaging for arrhythmias. Phys Med Biol. 2011c; 56:L1–L11.10.1088/0031-9155/56/22/F01 [PubMed: 22024555]

Provost J, Papadacci C, Arango JE, Imbault M, Fink M, Gennisson JL, Tanter M, Pernot M. 3D ultrafast ultrasound imaging in vivo. Phys Med Biol. 2014; 59:L1–L13.10.1088/0031-9155/59/19/L1 [PubMed: 25207828]

Provost J, Thiébaut S, Luo J, Konofagou EE. Single-Heartbeat Electromechanical Wave Imaging with Optimal Strain Estimation Using Temporally-Unequispaced Acquisition Sequences. Phys Med Biol. 2012; 57:1095–1112. [PubMed: 22297208]

Ramanathan C, Ghanem RN, Jia P, Ryu K, Rudy Y. Noninvasive electrocardiographic imaging for cardiac electrophysiology and arrhythmia. Nat Med. 2004; 10:422–428.10.1038/nm1011 [PubMed: 15034569]

Sysel P, Rajmic P. Goertzel algorithm generalized to non-integer multiples of fundamental frequency. EURASIP J Adv Signal Process. 2012; 2012:56.10.1186/1687-6180-2012-56

Tobón C, Ruiz-Villa CA, Heidenreich E, Romero L, Hornero F, Saiz J. A Three-Dimensional Human Atrial Model with Fiber Orientation. Electrograms and Arrhythmic Activation Patterns Relationship. PLoS ONE. 2013; 8:e50883.10.1371/journal.pone.0050883 [PubMed: 23408928]

Zhang Q, Yip GW-K, Yu C-M. Approaching regional left atrial function by tissue Doppler velocity and strain imaging. Europace. 2008; 10:iii62–iii69.10.1093/europace/eun237 [PubMed: 18955401]

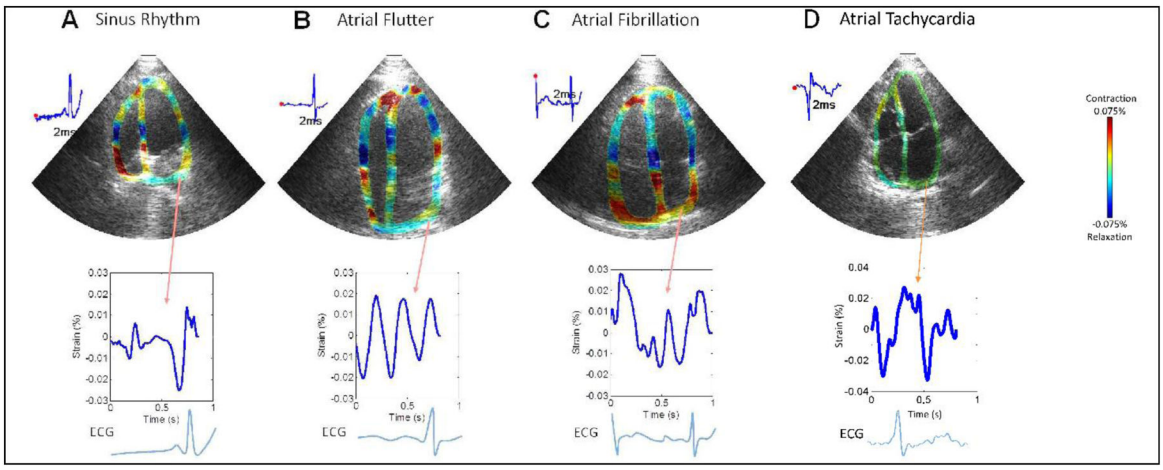

Figure 1.

Representative examples of high temporal resolution strains during different types of arrhythmia. A During sinus rhythm in a healthy volunteer, two main events can be observed during the cardiac cycle: end-systole, and end-diastole. By tracking the propagation front of the end-diastole electromechanical activation, one can obtain isochrones strongly correlated to electrical isochrones. B During atrial flutter, the strains are periodic. C During atrial fibrillation, the strains are chaotic and no period of zero strains are observed as in A. D. During focal tachycardia, distinct events, as in the case of sinus rhythm, can be observed. See corresponding supplementary video 1.

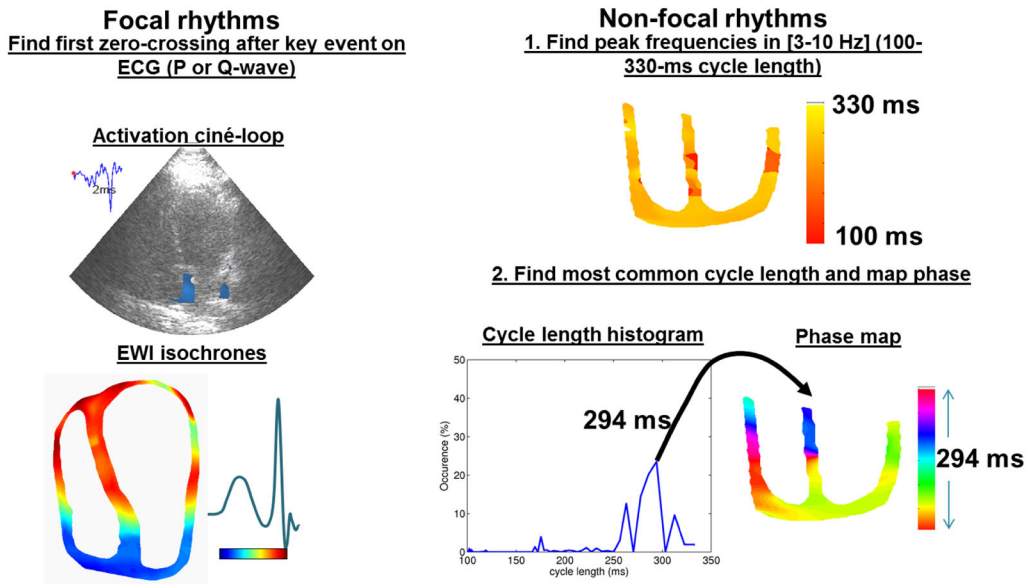

Figure 2.

Different processing for different types of rhythms. The electromechanical strains were processed differently whether the rhythm studied was focal or non-focal. For focal rhythms, the previously published EWI approach was used, i.e., the first time at which the strains crossed zero after the onset of the P-wave on the ECG was detected and displayed in the form of an activation ciné-loop and isochrones. For non-focal rhythms, the Fourier transform of the electromechanical strains in time was performed pixel-wise using a Goertzel algorithm. The peak frequencies located within 3 and 10 Hz were detected and mapped. In the case of atrial flutter, the phase map of the main peak frequencies was used to assess spatial propagation.

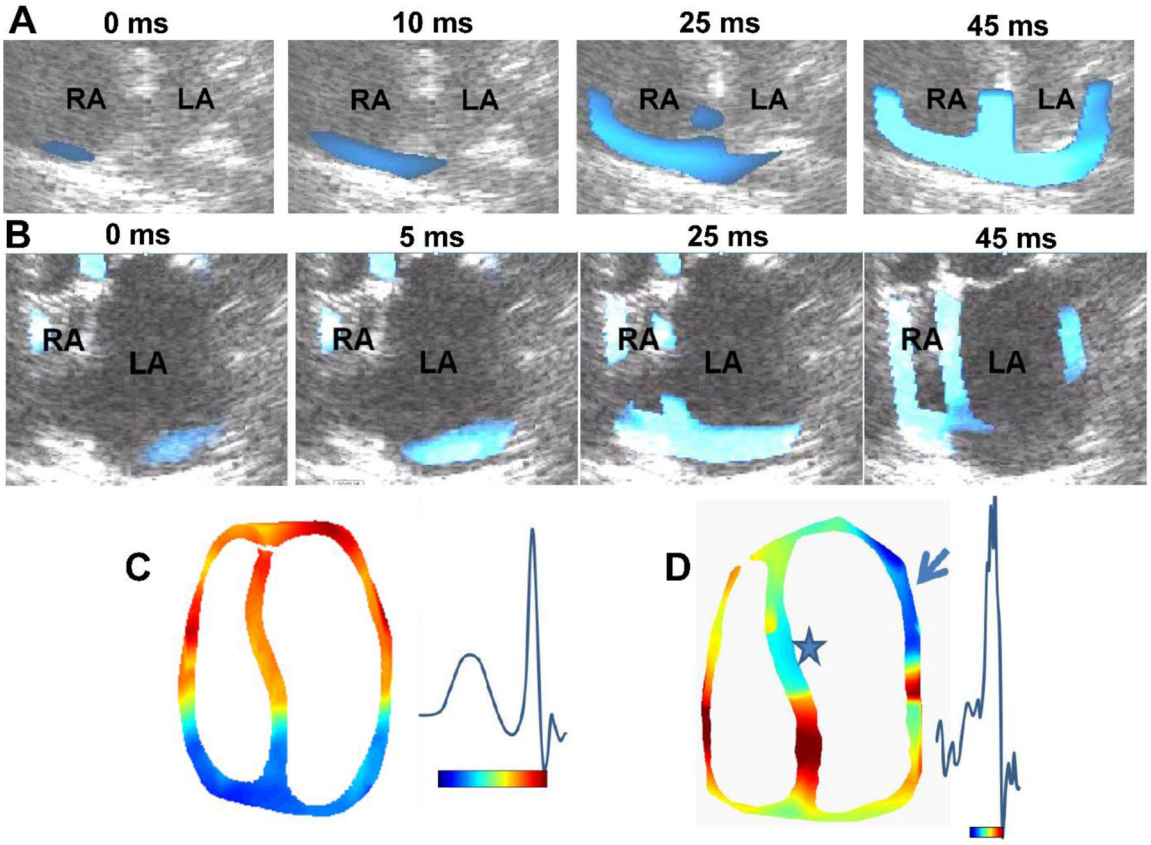

Figure 3.

Focal rhythm. A. Atria of a normal subject. The electromechanical activation depicted in blue originated in the right atrium and propagated towards the left atrium. B Atria of a patient undergoing focal atrial tachycardia with a focus suspected to be located high in the LA. The electromechanical activation depicted in blue originated high in the LA and propagated towards the left atria and the atrio-ventricular valves. C and D. Electromechanical isochrones of a ventricular tachycardia patient during C sinus rhythm and D premature ventricular complex. During sinus rhythm, activation originates in the RA and propagates into the LA and the ventricles, as previously shown in normal subjects. C. During premature ventricular complex, electromechanical activation originates from the lateral wall (arrow), and propagates toward the atria and into the atria. Note the early activation of the septum (star), indicating a potential recruitment of the Purkinje network. See corresponding supplementary video 2.

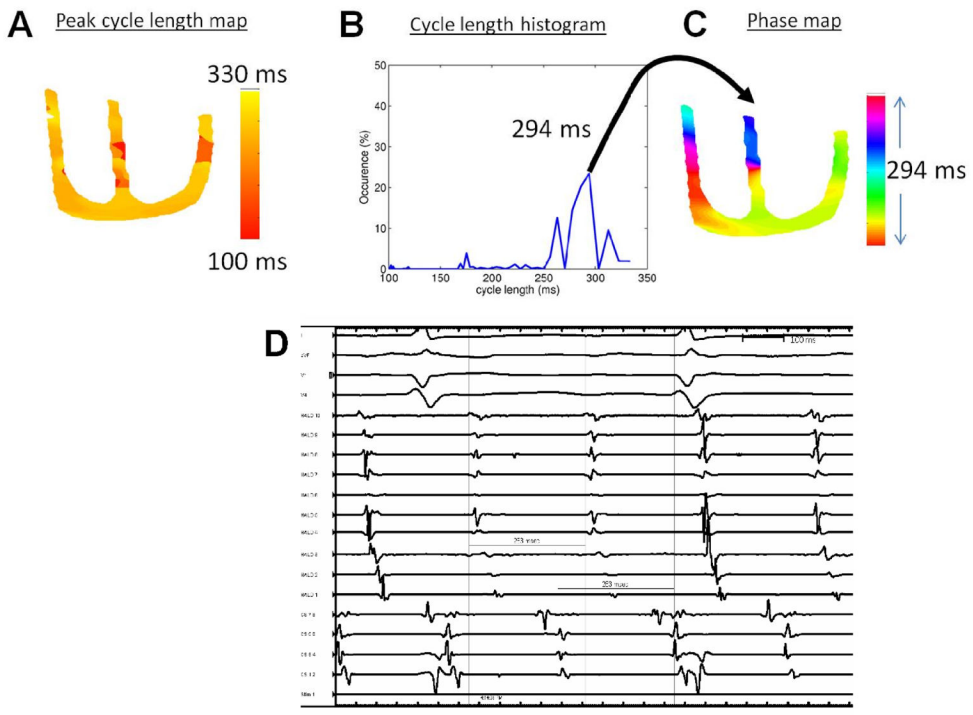

Figure 4.

Analysis of reentrant arrhythmias using a single-frequency atrial flutter case. A. The peak cycle length map indicates, for each pixel of the atria, which cycle length was most present in the Fourier spectrum. B The cycle length histogram can then be used to determine, among all the pixels of the atria, which cycle length represents best the atrial contraction. In the present case, one peak cycle length of 294 ms can clearly be identified. C The phase corresponding to the 294 ms cycle length can then be retrieved from the Fourier spectrum and used to map the propagation of the mechanical oscillation at 294 ms. While the phase cannot indicate where the activation started, the propagation direction can be determined; in this case, the electromechanical activation propagated from the RA to the LA. D Corresponding intracardiac electrogram obtained a few hours after the imaging procedure.

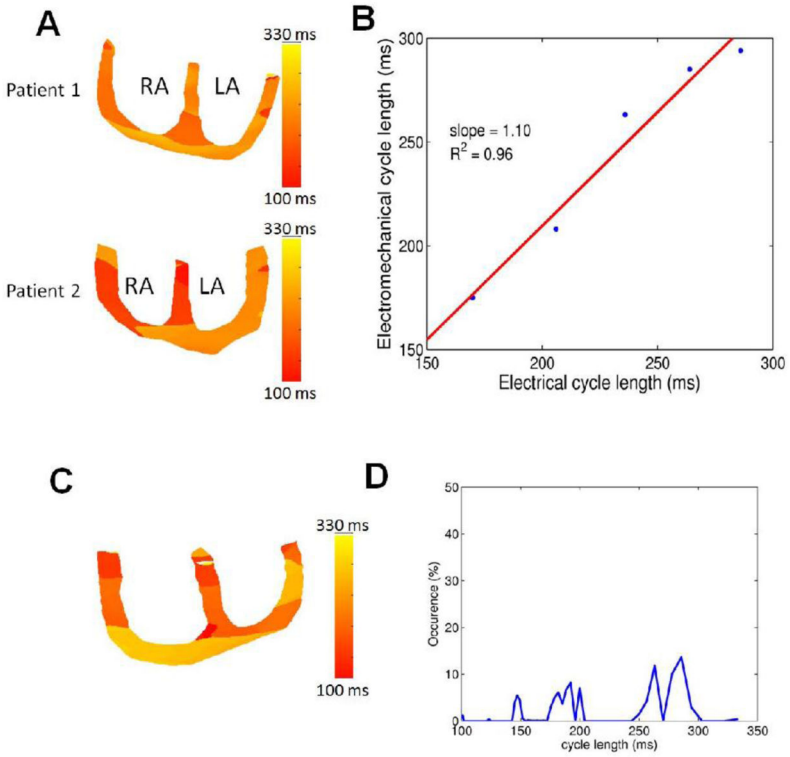

Figure 5.

A Peak cycle length map in two typical atrial flutter patients. Two dominant frequencies can be identified in each patient, with the shorter cycle length located in the RA. B Conducting this analysis in five patients, and choosing the peak cycle length closest to the electrical cycle length, one can obtain a strong correlation between the MCL and the electrical cycle length. C. The peak cycle length map during atrial fibrillation reveals further spatial fragmentation of the peak cycle length, as quantified by the associated histogram (D).